

Adsorption of cobalt (II) 5,10,15,20-tetrakis(2-aminophenyl)-porphyrin onto copper substrates: characterization and impedance studies for corrosion inhibition

Koodlur S. Lokesh^{a,1}, Michel De Keersmaecker^a, Alice Elia^a, Diederik Depla^b, Peter Dubruel^c, Peter Vandenaabeele^{a,d}, Sandra Van Vlierberghe^c and Annemie Adriaens^{a,*}

^a Department of Analytical Chemistry, Ghent University, Krijgslaan 281-S12, 9000 Ghent, Belgium

^b Department of Solid State Physics, Ghent University, Krijgslaan 281-S1, 9000 Ghent, Belgium

^c Department of Organic Chemistry, Ghent University, Krijgslaan 281-S4, 9000 Ghent, Belgium

^d Department of Archaeology, Ghent University, Sint-Pietersnieuwstraat 35, 9000 Ghent, Belgium

* To whom correspondence should be addressed.

E-mail: annemie.adriaens@ugent.be; Tel. +32 9 264 4826; Fax +32 9 264 4960

ABSTRACT

Molecular films of cobalt (II) 5,10,15,20-tetrakis(2-aminophenyl)-porphyrin have been deposited on a copper substrate by self-assembly. Characterization of the modified surface confirms the presence of a uniformly and homogeneously distributed film. In addition, Tafel plots show that the open circuit potential of the porphyrin modified copper electrode shifts towards a more positive value while the corrosion current density decreases by a magnitude of 10 times compared to the bare surface. Impedance data in 0.1 M sodium sulfate electrolyte show that the charge-transfer resistance of the modified copper reaches an inhibition efficiency of 97 %.

KEYWORDS

A: copper; A: organic coatings; B: electrochemical impedance spectroscopy; C: corrosion; C: inhibition

¹ Present address: Materials Chemistry, Shinshu University, Tokida, Ueda, Nagano, Japan

1 INTRODUCTION

Copper is an important metal in construction, chemical, electrical and electronic industries: its low bulk resistivity and excellent electromigration properties make it a suitable replacement for gold and aluminum in wafer metallization and wire bonding applications [1-2]. Due to the electrodisolution and corrosion of copper, there is a growing interest in the development of appropriate inhibitors for this metal.

Well-packed, orderly films which can be formed on the copper surface, must not only prevent the surface from corrosion but are also expected to support the ultrafine basic requirements anticipated for nano-sized electronic components [3]. The modified surface blocks the approach of electrochemically active species to the electrode surface, resulting in a complete suppression of their redox reactions at the electrode surface. The corrosion inhibition will be prominent in organic molecules due to their higher resistivity to electron transfer reactions [4-17]. They form a thin resistive layer on the metal surface and protect it from the surrounding reactive environment. The most studied organic molecules include alkanethiols, alkanolic acids, organosilanes, triazoles, amines, thiazoles, imidazoles, etc. When the molecules are short and micro-heterocyclic compounds, either electron tunneling across the thin films or penetration of electroactive species through defects, or both, allows the electrochemical reactions to proceed at the electrode. In order to overcome this problem, one should think of molecules that not only resist the electron transfer completely, but also can withstand extreme temperatures and are inert to the external atmosphere.

Macrocyclic complexes such as phthalocyanines and porphyrins are in this regard interesting compounds. These complexes are also well known for their thermal stability, chemical inertness and their behavior as an electron transfer mediator. In contrast to the latter, blocking effects can also be observed. The number of articles in the literature that describe the use of phthalocyanines and porphyrins as blocking agents are limited, but have been demonstrated for the corrosion inhibition of iron and steel [13-14, 18]. The adsorption and inhibiting abilities of these molecules are affected by factors and properties such as functional groups, steric influence, electron density profile at donor atoms and orbital character of donating compounds.

In the present study, we examine the formation of a cobalt (II) 5,10,15,20-tetrakis(2-aminophenyl)-porphyrin (Co(II)(T(o-NH₂))PP) film on a bare copper surface by chemisorption. The coated surface is characterized using different surface analysis techniques such as optical microscopy, Raman spectroscopy, X-ray photoelectron spectroscopy (XPS) and atomic force microscopy (AFM). The corrosion inhibition efficiency of the copper coated surface is measured using electrochemical impedance spectroscopy (EIS), linear polarization resistance (LPR) and Tafel analysis.

2 EXPERIMENTAL DETAILS

2.1 Materials

Co(II)(T(o-NH₂)PP) was purchased from Porphyrin Systems (Germany) and was used as such without any purification. Sodium sulfate and ethanol were purchased from Sigma-Aldrich. All the reagents were analytical grade. Double distilled water was used for the preparation of the Na₂SO₄ electrolyte solution. Circular copper coupons (purity 99.9 %) from Goodfellow Cambridge Ltd. of 12.5 mm diameter and 2 mm thickness were used for the characterization by optical microscopy, Raman spectroscopy, XPS and AFM. For the electrochemical measurements, electrodes in the form of inlaid copper disks with 2.0 mm diameter were used. They were embedded in an epoxy resin.

2.2 Sample preparation

The copper coupons and inlaid copper disks were polished using a polishing cloth (12" micro cloth PSA 10/PK, Buehler, Buehler) using sequentially 1.0 μm and 0.5 μm alumina. The electrodes were subsequently washed in water and later on in ethanol while being sonicated for 10 minutes in an ultrasonic bath. To minimize the exposure of the cleaned copper substrates to the air, the copper coupons were stored in a closed nitrogen atmosphere.

2.3 Formation of the chemisorbed film of Co(II)(T(o-NH₂)PP

The cleaned copper coupons and electrodes were immersed in a 1 mM Co(II)(T(o-NH₂)PP) solution, dissolved in ethanol for 24 h purged with N₂ to avoid the formation of an oxide layer, after which the samples were washed thoroughly with ethanol and water to remove the physically adsorbed material. The samples used for microscopy measurements, were partially covered with a standard adhesive tape (thickness 3 μm) in order to obtain a sample with both a Co(II)(T(o-NH₂)PP) modified and a bare copper surface.

2.4 Characterization of the modified surface

An optical microscope (Nikon SMZ 800 equipped with a Nikon Digital Sight system) was used to study the surface characteristics of the modified samples from a visual point of view. The microscope uses a Euromex fiber optic light source EK-1 to illuminate the copper sample. The images were recorded and analyzed using the software NIS Elements D 3.0 (Nikon).

A confocal Raman spectrometer Senterra R200-L (Bruker) was used to analyze the Co(II)(T(o-NH₂)PP) powder and the porphyrin coated copper sample. Raman spectra were recorded using a 785 nm diode laser with a power of 300 mW at the source. An Olympus microscope, coupled to the spectrometer, was used for the visualization of the sample and for the microanalysis with an objective lens of 50 x magnification. The spectrometer is equipped with a thermo-electrically cooled CCD detector (1024 x 256 pixels). Raman spectra were recorded in the wave number region of 100 – 1700

cm⁻¹ for the adsorbed film of porphyrin on the copper surface. For each spectrum 15 accumulations of 30 s were recorded.

XPS measurements were carried out using a S-Probe monochromatized XPS spectrometer from Surface Science Instruments (VG) with an Al K α X-ray (1486.6 eV) monochromatic source. The take off angle was 45° with the voltage and power of the source 10 kV and 200 W respectively. A base pressure of 2 x 10⁻⁹ mbar was obtained in the measuring chamber and the pass energy spectrum was 157.7 eV (resolution stand 4: 0.15 eV). The analysis surface was 250 x 1000 μ m² with a flood gun (neutralizer) setting of 0.2 eV. The accumulation time was about 3 h for Cu 2p and 1 h each for the N 1s, and C 1s spectra.

AFM images were obtained in ambient conditions with a multimode scanning probe microscope (Digital Instruments – USA) equipped with a Nanoscope IIIa controller. 10 μ m scans were recorded in tapping mode with a silicon cantilever (OTESPA – Veeco). The recorded images were modified with an X and Y plane fit auto procedure and then Nanoscope software version 4.43r8 was used for surface roughness analysis.

All the voltammetry experiments were performed using an Autolab potentiostat (PGSTAT 100, Netherlands) with GPES software, in a three-electrode cell system with saturated calomel electrode (SCE) as a reference electrode, a copper electrode modified with porphyrin as working electrode and carbon as counter electrode. The experiments were performed in a 0.1 M Na₂SO₄ electrolyte solution in an inert atmosphere by purging with nitrogen gas (Air Liquide Alphagaz 1 - accuracies from % to 10 ppm) during 20 minutes before each experiment. The linear polarization resistance technique (LPR) was used to study the corrosion inhibition behavior and the polarization resistance, R_p , of the Co(II)(T(o-NH₂)PP) adsorbed film on the copper surface. The LPR curves were recorded in a 0.1 M Na₂SO₄ solution in the potential range -20 to +20 mV with respect to the open circuit potential (OCP) at a scan rate of 1 mV/s. In addition, linear polarization and Tafel plots were used to determine the corrosion potential (E_{corr}) and corrosion current density (i_{corr}) for the bare as well as the modified surface. The potentiodynamic polarization curves were recorded in a potential window of -0.25 V to 0.25 V vs. OCP at a scan rate of 0.2 mVs⁻¹. Electrochemical impedance measurements were carried out using an Autolab potentiostat (PGSTAT 20, Netherlands) with the frequency response analysis (FRA) software, in the frequency range 100 kHz – 10 mHz with an amplitude of 5 mV. The aim was to study the charge transfer behavior of the bare and modified copper electrodes in a 0.1 M Na₂SO₄ solution at open circuit potential. The EIS data were fitted using the NOVA 1.5 software (Autolab, Netherlands).

3 RESULTS AND DISCUSSION

The structure of the cobalt (II) 5,10,15,20-tetrakis-(2-aminophenyl) porphyrin (Co(II)(T(o-NH₂)PP)) is shown in Figure 1. It has four amine groups at the ortho-position of the benzene ring and is soluble in

ethanol. The amine groups as well as aromatic π -electrons in the porphyrin ring are expected to interact with the copper surface to form a stable film. The stable film formation can also be attributed to the overlap between the d-orbital of the Co(II)-ion and the copper surface. A similar behavior was observed for silver and gold [19-21].

3.1 Surface characterization of the coated surface

Figure 2 shows the optical microscopy image for the Co(II)(T(o-NH₂)PP) modified copper surface (left) and the bare copper surface (right). It clearly shows the difference between both sides and the fact that the modified surface is uniformly and completely covered. A control experiment was also performed by dipping the bare copper surface in an ethanol solution saturated with N₂ to monitor the change in the surface. We were not able to observe any change, which clearly indicates that the modified surface is due to the adsorption of the porphyrin on the copper surface and not due to a reaction with the ethanol solvent.

Raman spectra of the bulk Co(II)(T(o-NH₂)PP) powder and the modified copper surface are given in Figure 3. The Raman signals of the two samples are in good agreement with data documented in the literature [22]. The spectra are dominated by strong in-plane stretching and breathing modes of the porphyrin aromatic and planar macrocycle and are assigned based on the reported literature [22]. Table 1 gives an overview of the various bands and their corresponding assignments. The stretching vibrations of the aromatic ring chain are observed at 1453 cm⁻¹ and 1564 cm⁻¹. The stretching vibration of the pyrrole ring on the porphyrin macrocycle is observed at 1338 cm⁻¹ and 1373 cm⁻¹. The macrocyclic vibration observed at 1077 cm⁻¹ can mainly be assigned to the ν (C=C). The pyrrole ring out-of-plane deformation is observed at 725 cm⁻¹ and the pyrrole ring breathing vibration appears at 751 cm⁻¹ [22-23]. The higher signal to noise ratio observed for the monolayer film (Figure 3b) can be explained by an ordered deposition of the porphyrin and by the surface enhancement effect of the Raman signal by the copper surface [24-26]. The metal-nitrogen band for the interaction between the nitrogen atom in the macrocycle group of the porphyrin and the cobalt atom is clearly seen in the bulk Co(II)(T(o-NH₂)PP) at around 250 cm⁻¹ [27-28]. The lower band intensity for the porphyrin on the copper surface can be explained by suggesting a transfer of electron density of the copper surface to the Co(II)-ion and thus the formation of a coordinative bond. This adsorption to the copper surface means that the interaction between the Co and N-atom decreases, which is observed in the Raman spectrum [29].

Figure 4 shows the core level X-ray photoelectron spectra for the Co(II)(T(o-NH₂)PP) film on the copper substrate. The different spectra show the C1s, N1s and Co2p peaks. The binding energy shift in the Co2p spectrum for the Co(II)(T(o-NH₂)PP) can be attributed to cobalt in the formal oxidation state +2. The Co2p_{3/2} peak appears at 780.8 eV and the Co2p_{1/2} peak is observed at 795.6 eV [30-31]. The Co2p_{3/2} signal shows two peaks due to a multiplet structure, which is caused by the unpaired electron in the d-shell of the Co(II)-ion (d⁷ electron structure) considering spin-orbit and electrostatic electron-

electron interactions [19]. This shift to a higher binding energy due to the +2 oxidation state of the cobalt atom can also explain the formation of a multilayer instead of a monolayer structure. The formation of a monolayer structure would suggest that the transfer of electron density is much larger for each individual Co(II)-ion in the porphyrin complex, which would show a bigger shift to a lower binding energy [32].

The C1s spectrum shows three contributions. The main peak at 284.7 eV is related to the aromatic carbon of the porphyrin molecules and phenyl rings. A shoulder peak at 286.8 eV can be assigned to C atoms connected to the N atoms of the peripheral amine group. A small third contribution at 289.6 eV is related to the π electrons in the aromatic rings. The ratio between the different peaks is probably distorted by an aliphatic C contamination, increasing the intensity of the 284.7 eV peak.

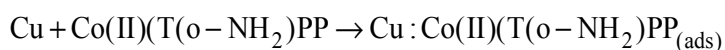
The N1s spectrum also shows three important contributions. Two major peaks in equal intensity are related to the nitrogen in the pyrrole position (at 398.2 eV) and in the amino group (399.3 eV) in the multilayer structure [33]. The peak at 400.6 eV is probably due to the nitrogen contamination by nitrogen (N_2) adsorption [24, 34].

Figure 5 shows the AFM images of the bare copper surface (Figures 5 a and c) and the Co(II)(T(o-NH₂)PP) modified copper surface (Figures 5 b and d). The top view (Figure 5c) shows that the deposited layer is completely and uniformly distributed on the surface, indicating that clusters of Co(II)(T(o-NH₂)PP) molecules cover the whole copper surface in an efficient way. The root mean square (RMS) roughness of the modified surface increased from 6 nm for bare copper to 30 nm for the porphyrin coated copper. The latter was anticipated since surface modification strategies always result in an increase in surface roughness [35]. The roughness increase after modification is clearly indicated in the 3D surface plots (see Figures 5c and 5d). All together the data clearly confirm the formation of a Co(II)(T(o-NH₂)PP) film, which is uniformly and homogeneously distributed on the copper surface.

3.2 Explanation of the film formation

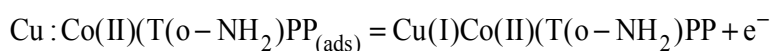
The interaction between Co(T(o-NH₂)PP) and the copper surface can be explained based on two types of interactions:

- 1) The porphyrin molecule has a benzotriazole like structure, which forms a complex with copper [5, 36-37]. The mechanism of the interaction of the porphyrin on the copper surface can be given by:



where $Cu : Co(II)(T(o-NH_2)PP)_{(ads)}$ stands for Co(II)(T(o-NH₂)PP) adsorbed on Cu surface.

In the presence of oxidants or by anodic polarization it can be oxidized to a protective complex:



Based on the porphyrin structure it can be seen that the molecule has two places convenient for bonding with the copper surface: the nitrogen atom with a lone sp^2 electron pair and the aromatic ring. The presence of nitrogen atoms in the pyrrole ring of the porphyrin enables bonding with

copper and is a basis for the inhibitive effect of porphyrin on the copper surface. Coordination between the porphyrin molecule and the copper surface occurs via the nitrogen atom of the pyrrole ring as reported for triazoles [38]. The benzotriazole like structure of the porphyrin is strongly adsorbed forming protective Cu(I) porphyrin compounds which effectively block and inhibit the corrosion in presence of an oxidant.

- 2) The electronic structure of the cobalt atom in the porphyrin complex shows a half-filled $3d(d_z^2)$ open-shell atomic orbital, which can bind most likely with the one electron in the Cu(4s) atomic orbital. Geometrically, the Co $3d_z^2$ orbital is oriented perpendicular to the porphyrin plane and is thus directed to the surface, which facilitates a good overlap. Electronically, this orbital is only singly occupied and represents both HOMO and LUMO (a SOMO) of the cobalt atom of the molecule, which means it can act as an electron donor and an acceptor [19]. The Cu-Co(T(o-NH₂)PP) interaction can thus be characterized as a simple two-electron, four spin-orbital interaction (or two-electron, two orbital interaction in closed-shell terminology), where the Co $3d_z^2$ overlaps with occupied states of the copper surface. The copper surface donates an electron to the porphyrin complex to form a covalent/coordinate bond. This means a monolayer of the porphyrin complex can be formed on the copper surface [33].

The cyclic conjugated porphyrin core system of the Co(II)(T(o-NH₂)PP) molecule is a rich electron ring with a high electronic density and therefore undergoes a saddle-shape distortion and will not stay in its expected planar geometry when reacting with the copper surface. The peripheral phenyl rings of the porphyrin rotate towards the molecular plane, because of steric repulsions between the phenyl rings and the Cu surface [39].

The first interaction pulls away the electron density from the porphyrin ring due to the interaction of the copper surface with the π -electrons and the electron pairs of the nitrogen atoms. The second interaction uses electrons from the copper surface to interact with the cobalt metal center of the porphyrin. This means both interactions are needed to produce a strong bonding with the copper surface (see Figure 6).

After the formation of this distorted monolayer on the copper surface, the formation of a multilayer starts. An indication of this multilayer are the bright dots, observed in the AFM images (Figure 5), attributed initially to the aggregated islands of Co(II)(T(o-NH₂)PP), which form a square unit cell of a lattice in the multilayer induced by the substrate/adsorbate interactions [40]. The islands and the lattice are formed due to the compression because of a considerable tilt angle of the individual porphyrins in the multilayer, i.e. the porphyrin plane is not parallel with the surface. The angle tilt could be caused by specific interactions between the molecules in the top layer or by a rough topography of the first layer, which serves as a substrate for the multilayer [40]. The best way to explain this multilayer formation is to assume an attractive lateral interaction between the different self-assembled layers of the porphyrin complex. The driving force of this self-assembly in well-ordered domains relies on intermolecular interactions. Two types of attractive interactions of the

phenyl rings of the TPPs (tetraphenyl porphyrin) appear to be likely, namely π - π stacking or T-stacking, which also plays a key role in biological recognition. This means the phenyl groups of the individual porphyrins are either parallel (π - π) or perpendicular (T-type) to each other [40].

This theory can be verified by the XPS and Raman measurements. The XPS measurements show a multiplet structure for the Co(II) atom and no shift in the C-N pyrrole functions, which indicates a multilayer is formed on the surface [19]. The Raman spectrum of the porphyrin coated copper surface shows sharp and high peaks for the Raman shifts of the macrocycle of the porphyrin. The stacking interactions between the different macrocycles provide not only an increased polarizability and thus an enhancement of the Raman signal, but also shift the peaks of the macrocycle a little bit compared to the bulk [41].

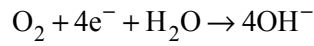
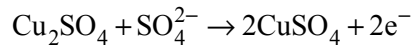
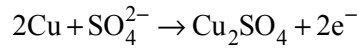
The inhibition action is a result of the adsorption and multilayer formation of the porphyrin complex on the copper surface forming a blocking barrier to copper corrosion. The formation of this multilayer provides an enhanced electrical resistance at the copper surface. The corrosion inhibition efficiency observed with the porphyrin film is thus mainly due to (1) the adsorption of the Co(II)- porphyrin complex on the metal surface and the transfer of electrons between the open-shell orbital of the porphyrin complex inhibitor and the metal orbital and (2) the formation of a porphyrin multilayer.

3.3 Examination of the corrosion inhibition

The Tafel plots for the bare copper and the Co(II)(T(o-NH₂)PP) modified copper surface recorded in a 0.1 M Na₂SO₄ electrolyte solution are shown in Figure 7. They demonstrate that the open circuit potential for the porphyrin-modified electrode has shifted towards a slightly more positive potential compared to the bare copper electrode (~ 45 mV). As expected, both the anodic and cathodic corrosion reactions are inhibited remarkably using the porphyrin-modified surface. The corrosion current density (i_{corr}) has been calculated using the Tafel slopes, as shown in Figure 7. The slopes were determined in the Tafel region of the anodic and cathodic curves approximately 40 mV before and after the corrosion potential. The i_{corr} value obtained for the bare copper electrode is $5.98 \times 10^{-7} \text{ A cm}^{-2}$, with a relative standard deviation (RSD) of 12 %, and decreases to $6.38 \times 10^{-8} \text{ A cm}^{-2}$ (RSD 26 %) for the modified copper surface. The i_{corr} values are derived from averaging the values from four experiments. The measured polarization resistance (R_p) increases from $9.88 \times 10^2 \Omega \text{ cm}^2$ (RSD 18 %) for bare copper to $1.34 \times 10^4 \Omega \text{ cm}^2$ (RSD 21 %) for the modified copper surface.

The lower corrosion current density and the higher polarization resistance indicate that the porphyrin film on a copper electrode reduces the dissolution rate of copper in a 0.1 M Na₂SO₄ electrolyte solution and therefore protects the copper surface effectively. This implies that porphyrin layers can inhibit copper corrosion. The latter is due to the resistive behavior of the porphyrin layer formed on the surface, which can be explained on the basis of the interaction between the vacant d-orbital of the copper and the π -electrons of the macrocycle.

A Nyquist plot and Bode plot for the bare and the modified copper are shown in Figure 8. One can consider the following electrochemical corrosion reactions in the cell [42-43]:



The Nyquist plot ($Z_{\text{imaginary}}$ versus Z_{real}), in Figure 8a, exhibits the characteristic semicircles at high frequencies and a straight line at low frequencies, corresponding to kinetic and diffusion processes happening at the electrode. The slightly depressed nature of the semicircles, even for the bare copper electrode, indicates impedance dispersion. This can be explained by the time constant distribution of more than one electrochemical process happening at the electrode surface and by the roughness of the electrode surface and/or the non-uniform distribution of the current density at the surface [44-45]. The diameter of the semicircle is approximately equivalent to the value of the charge-transfer resistance (R_{ct}) of the corrosion process and is associated with the corrosion inhibition ability of the film. The charge-transfer resistance of the Co(II)(T(o-NH₂)PP) covered electrode is larger than that of the bare electrode, which indicates that the presence of the Co(II)(T(o-NH₂)PP) film blocked the transfer of the electrons from the copper surface to the solution and accordingly protects the surface from corrosion effectively.

The phase angle plot of the bare copper (Figure 8b) shows one time constant related to the native Cu₂O copper (I) oxide layer. The two maximums of the treated copper surface indicate the presence of two different time constants in the Bode plot. The first time constant, at the low frequency range, is related to the Cu₂O layer, which is not removed before coating our copper surface and the second time constant, at an intermediate frequency range shows a higher phase angle and is related to the Co(II)(T(o-NH₂)PP) film. This indicates the better protective behavior of the Co(II)(T(o-NH₂)PP) film enhancing the protection afforded by the native Cu₂O layer.

The higher impedance values observed in Figure 8c for the modified copper electrode indicate that the modified porphyrin layer is highly protective compared to the bare copper metal.

To fit the EIS data recorded at the OCP potential, the spectra were modeled using the Randles' equivalent circuits of mixed kinetic and diffusion control as shown in Figure 9, taking into account the number of time constants deduced from the phase angle plot. Figure 9a shows the Randles' circuit with one time constant where R_s is the resistance of the electrolyte, Q_{dl} is the constant phase element representing the double layer, R_{ct} is the electron-transfer resistance (domain of kinetic control) representing the most appropriate parameter to monitor the protective properties of the film and W is the Warburg impedance (domain of mass transport control) [46]. Figure 9b shows an electric circuit with two time constants where Q_{coat} is the constant phase element, which represents the Co(II)(T(o-NH₂)PP) film capacitance and a resistor R_{coat} represents the pore resistance of the coating due to the

presence of copper(I)oxide. The second time constant can be explained by the presence of defects in the porphyrin layer due to the presence of the copper (I) oxide layer, which makes it more difficult to produce a pore free protective film. Constant phase elements instead of pure capacitors were used because the copper (I) oxide layer is a non-ideal dielectric and forms a gradient of conductivity through the oxide layer. Other explanations are the surface roughness, the varying thickness of the film and a non-uniform current distribution. The constant phase element (CPE), Q , consists of two parameters, Y_o and n , respectively, the numerical value of the admittance at $\omega = 1$ rad/s and $-(90.n)^\circ$ the phase angle of the CPE. The CPE behavior for macrocyclic porphyrin molecules modified electrodes has been reported earlier [47-48]. The estimated EIS parameters obtained using these two electric circuit models are presented and summarized in Table 2. The Nyquist plot (a) and the Bode plots (b and c) in Figure 8 show that the simulated plots based on our previous stated models agree well with the experimentally obtained results.

It is well known that in 0.1 M Na_2SO_4 solution copper easily forms a copper (I) oxide layer, which means diffusion due to a concentration difference can take place through a thin Cu_2O film. This diffusion is much stronger for a bare copper electrode than for a porphyrin coated copper sample (see Table 2). This can be explained by assuming a thicker film (d) due to the porphyrin coating, which means the double layer capacitance C_{dl} becomes smaller using the definition of the parallel-plate capacitance (see also Table 2) [44]:

$$C_{dl} = \frac{\epsilon\epsilon_0 A}{d}$$

where ϵ_0 is the permittivity of the vacuum, ϵ is the permittivity of the coating layer, A is the surface and d is the thickness of the coating.

A smaller capacitance predicts a smaller charge on the coating/electrolyte interface and therefore a smaller concentration difference in the electrolyte solution and of course less diffusion of ions [49]. The presence of the Warburg impedance in the electrochemical equivalent circuit model is also an indication of the porous nature of the modified surface [24, 50]. The slope of the Nyquist plot of the bare copper sample at low frequency is -0.5 , which also strongly indicates an infinite diffusion process at the electrode.

The increase in charge-transfer resistance R_{ct} for the modified electrode can be explained by an increase of the resistive behavior attained by the electrode on modification with the porphyrin. This means the porphyrin modification leads to a higher protection of the copper surface than the native copper(I) oxide layer. The pore resistance R_{coat} becomes finite, which means that the copper electrode has been subjected to corrosion or is currently undergoing corrosion at the metal/coating interface. The electrolyte can reach the existing corrosion layer through pores in the porphyrin layer and can attack the bare copper underneath to form a bigger corrosion layer.

Comparing both double layer capacitances, C_{dl} of the bare copper and the porphyrin coated sample shows that the C_{dl} for bare copper is much higher. The high C_{dl} indicates a poorly protective oxide

layer is or had been formed on the copper surface. The lower C_{dl} due to the Co(II)(T(o-NH₂))PP film can be explained by the better protection of the copper metal and the higher charge-transfer resistance. The capacitance of the porphyrin coating C_{coat} is almost equal to the capacitance of the double layer C_{dl} . The tiny difference suggests a thin porphyrin film covering the copper electrode with the copper (I) oxide layer. The n-values are approximately 0.53 for bare copper, which indicates a non-ideal dielectric oxide layer and a decrease in capacitive behavior. The n-value for C_{coat} is 0.85 for the coated copper suggests an almost ideal capacitive behavior of the porphyrin film and therefore a well-protective barrier. The I (inhibition efficiency), expressed in %, is related to θ , the degree of the porphyrin film coverage and is defined by:

$$I(\%) = \theta \cdot 100$$

The film coverage is calculated by the ratio of the charge transfer resistance of the bare and the modified surface [40]. The coverage (θ) of the film is defined using the following expression:

$$\theta = \frac{R_{ct} - R_{ct}^0}{R_{ct}}$$

R_{ct}^0 and R_{ct} represent the charge-transfer resistance of the bare electrode and porphyrin modified electrode. The inhibition efficiency is calculated to be 97.94 % with a standard deviation of ± 2 %, which is much higher than the reported values for other porphyrins in the literature [19].

Though the shift in the potential, polarization resistance and corrosion current density are comparatively less, these preliminary results are encouraging and can be used to improve the corrosion inhibition by varying the experimental conditions and/or the macrocycle (porphyrin, phthalocyanine or dendrimer) with different functional groups and metal ions. Further research is needed to optimize this change in R_p and i_{corr} .

4 CONCLUSIONS

A molecular film of cobalt (II) 5,10,15,20-tetrakis(2-amino-phenyl)-porphyrin Co(II)(T(o-NH₂))PP was successfully chemisorbed on a copper surface for the first time. Optical microscopy, Raman spectroscopy, XPS, AFM, LPR and electrochemical impedance spectroscopy showed the formation of a well-ordered multilayer film on the surface. The chemical adsorption is due to the strong interaction between aromatic π -electron of the porphyrin and copper surface and also due to the overlap of the d-orbital of the Co(II)-ion center of the porphyrin complex and the copper surface. The multilayer formation provides a higher corrosion resistance and a good corrosion protection. Tafel plots show a decrease in the corrosion current density i_{corr} value for the modified electrode compared to bare copper surface. The porphyrin molecules provide an inhibition efficiency of ca. 97 % and cover almost the entire copper surface. The charge-transfer resistance of the porphyrin covered electrode is nearly 80 times higher than that of the bare electrode, which indicates that the presence of the porphyrin film

blocks a part of the electron-transfer from the copper surface to the solution and accordingly protect the surface from corrosion.

ACKNOWLEDGEMENTS

The authors are thankful to N. De Roo, S. Lycke and T. Desmet for helping with the actual measurements. K.S. Lokesh and A. Elia are grateful to respectively Ghent University and the Research Foundation-Flanders (FWO, Belgium) for their postdoctoral and doctoral fellowship. Financial support of the Belgian Science Policy - Interuniversity Attraction Poles program P6/16 (Belgian State) is greatly acknowledged. K. De Wael is acknowledged for proof reading the manuscript in its early stage.

REFERENCES

- [1] C. Whelan, M. Kinsella, L. Carbonell, H.M. Ho, K. Maex, Corrosion inhibition by self-assembled monolayers for enhanced wire bonding on Cu surfaces, *Microelectron. Eng.* 70 (2003) 551-557.
- [2] J. Rickerby, J.H.G. Steinke, Current trends in patterning with copper, *Chem. Rev.* 102 (2002) 1525-1550.
- [3] D.T. Rooney, N.T. Castello, M. Cibulsky, D. Abbott, D. Xie, Materials characterization of the effect of mechanical bending on area array package interconnects, *Microelectron. Int.* 20 (2003) 34-42.
- [4] R. Ravichandran, R. Nanjundan, N. Rajendran, Effect of benzotriazole derivatives on the corrosion of brass in NaCl solutions, *Appl. Surf. Sci.* 236 (2004) 241-250.
- [5] M. Finšgar, I. Milošev, Inhibition of copper corrosion by 1,2,3-benzotriazole: a review, *Corros. Sci.* 52 (2010) 2737-2749.
- [6] A. Igual Muñoz, J. García Antón, J.L. Guiñón, V. Pérez Herranz, V. Comparison of inorganic inhibitors of copper, nickel and copper–nickels in aqueous lithium bromide solution, *Electrochim. Acta* 50 (2004) 957-966.
- [7] E.M. Sherif, Su-Moon Park, 2-Amino-5-ethyl-1,3,4-thiadiazole as a corrosion inhibitor for copper in 3.0% NaCl solutions, *Corros. Sci.* 48 (2006) 4065-4079.
- [8] G. Vastag, E. Szócs, A. Shaban, I. Bertóti, K. Popov-Pergal, E. Kálmán, Adsorption and corrosion protection behavior of thiazole derivatives on copper surfaces, *Solid State Ionics* 141-142 (2001) 87-91.
- [9] C. Öğretir, S. Çaliş, G. Bereket, H. Berber, A theoretical search on metal-ligand interaction mechanism in corrosion of some imidazolidine derivatives, *J. Mol. Struct. Theochem.* 626 (2003) 179-186.

- [10] M. Özcan, İ. Dehri, Electrochemical and quantum chemical studies of some sulphur-containing organic compounds as inhibitors for the acid corrosion of mild steel, *Prog. Org. Coat.* 51 (2004) 181-187.
- [11] D. Heim, K. Seufert, W. Auwärter, C. Aurisicchio, C. Fabbro, D. Bonifazi, J.V. Barth, Surface-assisted assembly of discrete porphyrin-based cyclic supramolecules, *Nano Lett.* 10 (2010) 122-128.
- [12] N. Lin, S. Stepanow, F. Vidal, K. Kern, M.S. Alam, S. Strömsdörfer, V. Dremov, P. Müller, A. Landa, M. Ruben, Surface-assisted coordination chemistry and self-assembly, *Dalton Trans.* 23 (2006) 2794-2800.
- [13] I.V. Aoki, I.G. Guedes, S.L. Maranhao, Copper phthalocyanine as corrosion inhibitor for ASTM A606-4 steel in 16% hydrochloric acid, *J. Appl. Electrochem.* 32 (2002) 915-919.
- [14] P. Zhao, Q. Liang, Y. Li, Electrochemical, SEM/EDS and quantum chemical study of phthalocyanines as corrosion inhibitors for mild steel in 1 mol/l HCl, *Appl. Surf. Sci.* 252 (2005) 1596-1607.
- [15] D-Q. Zhang, L-X. Gao, Q-R. Cai, K.Y. Lee, Inhibition of copper corrosion by modifying cysteine self assembled film with alkylamine/alkylacid compounds, *Mater. Corros.* 61 (2010) 16-21.
- [16] D.A. Hutt, C. Liu, Oxidation protection of copper surfaces using self-assembled monolayers of octadecanethiol, *Appl. Surf. Sci.* 252 (2005) 400-411.
- [17] Y. Tan, M. Mocerino, T. Paterson, Organic molecules showing the characteristics of localised corrosion aggravation and inhibition, *Corros. Sci.* 53 (2011) 2041-2045.
- [18] Y. Feng, S. Chen, W. Guo, G. Liu, H. Ma, L. Wu, Electrochemical and molecular simulation studies on the corrosion inhibition of 5,10,15,20-tetraphenylporphyrin adlayers on iron surface, *Appl. Surf. Sci.* 253 (2007) 8734-8742.
- [19] T. Lukasczyk, K. Flechtner, L.R. Merte, N. Jux, F. Maier, J.M. Gottfried, H.P. Steinrück, Interaction of cobalt(II) tetraarylporphyrins with a Ag(111) surface studied with photoelectron spectroscopy, *J. Phys. Chem. C* 111 (2007) 3090-3098.
- [20] F. Buchner, F. Flechtner, Y. Bai, E. Zillner, I. Keller, H.P. Steinrück, H. Marbach, J.M. Gottfried, Coordination of iron atoms by tetraphenylporphyrin monolayers and multilayers on Ag(111) and formation of iron-tetraphenylporphyrin, *J. Phys. Chem. C* 112 (2008) 15458-15465.
- [21] L. Scudiero, D.E. Barlow, K.W. Hipps, Physical properties and metal ion specific scanning tunneling microscopy images of metal(II) tetraphenylporphyrins deposited from vapor onto gold (111), *J. Phys. Chem. B* 104 (2000) 11899-11905.
- [22] R.S. Czernuszewicz, E.M. Maes, J.G. Rankin, *Porphyrin Handbook*, Vol 7, Theoretical and physical characterization; Resonance Raman spectroscopy of petroporphyrins (Eds., K.M. Kadish, K.M. Smith, R. Guilard), Academic Press, 2000, 293-338.

- [23] I. Gallardo, J. Pinson, N. Vila, Spontaneous attachment of amines to carbon and metallic surfaces, *J. Phys. Chem. B* 110 (2006) 19521-19529.
- [24] K.S. Lokesh, K. De Wael, A. Adriaens, Self-assembled supramolecular array of polymeric phthalocyanine on gold for the determination of hydrogen peroxide, *Langmuir* 26 (2010) 17665-17673.
- [25] K.S. Lokesh, N. Venkata, S. Sampath, Phthalocyanine macrocycle as stabilizer for gold and silver nanoparticles, *Microchim. Acta* 167 (2009) 97-102.
- [26] C.A. Jennings, G.J. Kovacs, R. Aroca, Near-infrared surface-enhanced Raman scattering from metal island films, *J. Phys. Chem.* 96 (1992) 1340-1343.
- [27] D. Dobrzyńska, J. Janczak, A. Wojciechowska, K. Helios, Structure and spectroscopic study of a novel complex: Tetrakis(benzimidazole)(perchlorato)copper(II)(perchlorate) hemihydrate, *J. Molecul. Struc.* 973 (2010) 62-68.
- [28] E. Faulques, D.L. Perry, S. Lott, J.D. Zubkowski, E.J. Valente, Study of coordination and ligand structure in cobalt-EDTA complexes with vibrational microspectroscopy, *Spectrochim. Acta A* 54 (1998) 869-878.
- [29] S.N. Terekhov, S.G. Kruglik, V.L. Malinovskii, V.A. Galievsky, V.S. Chirvony P.-Y. Turpin, Resonance Raman characterization of cationic Co(II) and Co(III) tetrakis(*N*-methyl-4-pyridinyl) porphyrins in aqueous and non-aqueous media, *J. Raman Spec.* 34 (2003) 868-881.
- [30] T.J. Chuang, C.R. Brundle, D.W. Rice, Interpretation of the X-ray photoemission spectra of cobalt oxides and cobalt oxide surfaces, *Surf. Sci.* 59 (1976) 413-429.
- [31] A. Mekki, D. Holland, Kh. Ziq, C.F. McConville, XPS and magnetization studies of cobalt sodium silicate glasses, *J. Non-Cryst. Solids* 220 (1997) 267-279.
- [32] K. Flechtner, A. Kretschmann, H.P. Steinrück, J.M. Gottfried, NO-induced reversible switching of the electronic interaction between a porphyrin-coordinated cobalt ion and a silver surface, *J. Am. Chem. Soc.* 129 (2007) 12110-12111.
- [33] Y. Bai, M. Sekita, M. Schmid, T. Bischof, H.P. Steinrück, J.M. Gottfried, Interfacial coordination interactions studied on cobalt octaethylporphyrin and cobalt tetraphenylporphyrin monolayers on Au(111), *Phys. Chem. Chem. Phys.* 12 (2010) 4336-4344.
- [34] D.H. Karweik, N. Winograd, Nitrogen charge distributions in free-base porphyrins, metalloporphyrins, and their reduced analogs observed by X-ray photoelectron spectroscopy, *Inorg. Chem.* 15 (1976) 2336-2342.
- [35] C.D. Gu, H. Ren, J.P. Tu, T.Y. Zhang, Micro/nanobinary structure of silver films on copper alloys with stable water-repellent property under dynamic conditions, *Langmuir* 25 (2009) 12299-12307.
- [36] A.M. Abdullah, F.M. Al-Kharafi, B.G. Ateya, Intergranular corrosion of copper in the presence of benzotriazole, *Scripta Materialia* 54 (2006) 1673-1677.

- [37] M.M. Antonijevic, M.B. Petrovic, Copper corrosion inhibitors. A review, *Int. J. Electrochem. Sci.* 3 (2008) 1-28.
- [38] R. Subramanian, V. Lakshminarayanan, Effect of adsorption of some azoles on copper passivation in alkaline medium, *Corros. Sci.* 44 (2002) 535-554.
- [39] W. Hieringer, K. Flechtner, A. Kretschmann, K. Seufert, W. Auwärter, J.V. Barth, A. Görling, H.P. Steinrück, J.M. Gottfried, The surface trans effect: influence of axial ligands on the surface chemical bonds of adsorbed metalloporphyrins, *J. Am. Chem. Soc.* 133 (2011) 6206-6222.
- [40] F. Buchner, I. Kellner, W. Hieringer, A. Görling, H.P. Steinrück, H. Marbach, Ordering aspects and intramolecular conformation of tetraphenylporphyrins on Ag(111), *Phys. Chem. Chem. Phys.* 12 (2010) 13082-13090.
- [41] S. Miljanić, A. Dijanošić, I. Piantanida, Z. Meić, M.T. Albelda, A. Sornosa-Ten, E. García-Espana, Surface-enhanced Raman study of the interactions between tripodal cationic polyamines and polynucleotides, *Analyst* 136 (2011) 3185-3193.
- [42] E. Hamed, Studies of the corrosion inhibition of copper in Na₂SO₄ solution using polarization and electrochemical impedance spectroscopy, *Mater. Chem. Phys.* 121 (2010) 70-76.
- [43] M. Scendo, Corrosion inhibition of copper by purine or adenine in sulphate solutions, *Corros. Sci.* 49 (2007) 3953-3968.
- [44] S. Hettiarachichi, Y.W. Chan, R.B. Wilson Jr., V.S. Agarwala, Macrocyclic corrosion inhibitors for steel in acid chloride environments, *Corrosion* 45 (1989) 30-34.
- [45] A. Amirudin, D. Thierry, Application of electrochemical impedance spectroscopy to study the degradation of polymer-coated metals, *Progr. Org. Coat.* 26 (1995) 1-28.
- [46] S.L.A. Maranhao, I.C. Guedes, F.J. Anaissi, H.E. Toma, I.V. Aoki, Electrochemical and corrosion studies of poly(nickel-tetraaminophthalocyanine) on carbon steel, *Electrochim. Acta* 52 (2006) 519-536.
- [47] M.J. Rodriguez Presa, R.I. Tucceri, M.I.; Florit, D. Posadas, Constant phase element behavior in the poly(o-toluidine) impedance response, *J. Electroanal. Chem.* 502 (2001) 82-90.
- [48] S. Mitra, K.S. Lokesh, S. Sampath, Exfoliated graphite–ruthenium oxide composite electrodes for electrochemical supercapacitors, *J. Power Sources* 185 (2008) 1544-1549.
- [49] K.I. Ozoemena, T. Nyokong, D. Nkosi, I. Chambrier, M.J. Cook, Insights into the surface and redox properties of single-walled carbon nanotube—cobalt(II) tetra-aminophthalocyanine self-assembled on gold electrode, *Electrochim. Acta* 52 (2007) 4132-4143.
- [50] C. Liang, P. Wang, B. Wu, N. Huang, Inhibition of copper corrosion by self assembled monolayers of triazole derivatives in chloride-containing solution, *J. Solid State Electrochem.* 14 (2010) 1391-1399.

Table 1. Raman spectral bands of Co(II)(T(o-NH₂)PP) film on copper, with their respective assignments [22-23].

Raman shift, cm ⁻¹	Assignments
1564	ν (C _{β} C _{β} + C _{α} C _m)
1511	ν (C _{α} C _m) _{sym}
1453	ν (C _{β} C _{β})
1373	ν (C _{α} C _{β}), ν (C _{β} C _s), ν (pyr half-ring) _{sym}
1338	ν (pyr half-ring) _{sym}
1247	δ (C _m H)
1149	δ (pyr)
1077	ν (C _{β} C _{β}) _{asym}
1014	ν (C _{β} C _{β}) _{asym}
820	ν (pyr breathing)
751	ν (pyr breathing)
725	δ (pyr def) _{sym}
693	δ (pyr def) _{sym}
641	δ (por)
595	δ (pyr def) _{asym}
536	δ (pyr rot)
360	δ (pyr rot) + ν (Co-N)
250	δ (C _{β} C _{β}) _{sym} + ν (Co-N)
	ν , Stretching; δ , Bending

Table 2. Summary of estimated EIS parameters obtained for the electrodes at the open circuit potential (vs. SCE).

Electrodes	R_s (Ω .cm ²)	R_{ct} (Ω .cm ²)	C_{dl} (μ F/cm ²)	W (Ω s ^{-1/2})	C_{coat} (μ F/cm ²)	R_{coat} (Ω .cm ²)
Bare Cu	4.66	37.68	39.04 (8)	0.0047	-	-
Cu-Co(II)(T(o-NH ₂)PP)	5.37	2922.51	10.71	0.000064	8.34	66.39

Figure Captions

- Fig. 1. Structure of 5,10,15,20-tetrakis-(2-aminophenyl) porphyrin-cobalt(II), (Co(II)(T(o-NH₂)PP)).
- Fig. 2. Optical microscopy image at the cross-section of the modified and bare copper surface.
- Fig. 3. Raman spectra of (a) Co(II)(T(o-NH₂)PP) as bulk sample and (b) Co(II)(T(o-NH₂)PP) modified copper surface.
- Fig. 4. X-ray photoelectron spectra of (a) carbon 1s, (b) nitrogen 1s and (c) cobalt 2p regions for the Co(II)(T(o-NH₂)PP) film on copper.
- Fig. 5. AFM images (a) top view, (b) 3D surface for the bare copper surface and (c) top view, (d) 3D surface for the Co(II)(T(o-NH₂)PP) modified copper surface.
- Fig. 6. The interaction of the porphyrin molecule with the copper surface. The arrows explain the electron density shifts and bond formation of both interactions.
- Fig. 7. Tafel plots for (a) the bare copper electrode and (b) the Co(II)(T(o-NH₂)PP) modified copper electrode in 0.1 M sodium sulfate solution at the open circuit potential. The thin tangential lines indicate the Tafel slopes.
- Fig. 8. (a) Nyquist plot, (b) Bode phase plot and (c) log(Z) vs log (f) plot for (i) the bare copper electrode and (ii) the Co(II)(T(o-NH₂)PP) modified copper electrode, in a 0.1 M sodium sulfate solution at the open circuit potential.
- Fig. 9. Equivalent circuit for the copper modified electrode: (a) two-time constant model and (b) simplified Randles equivalent circuit.

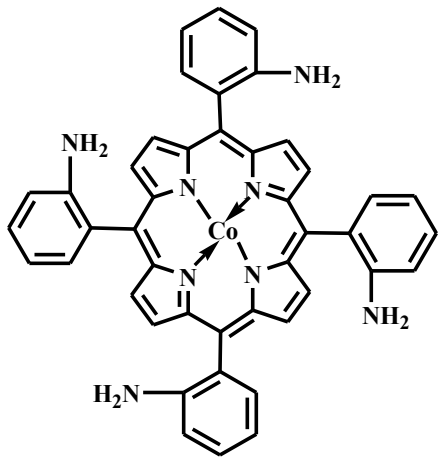


Figure 1

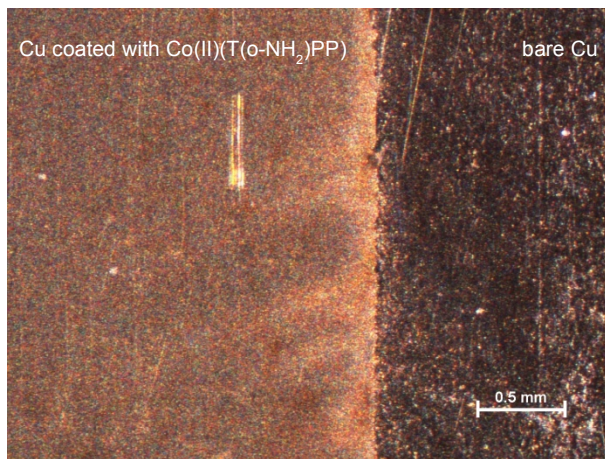


Figure 2

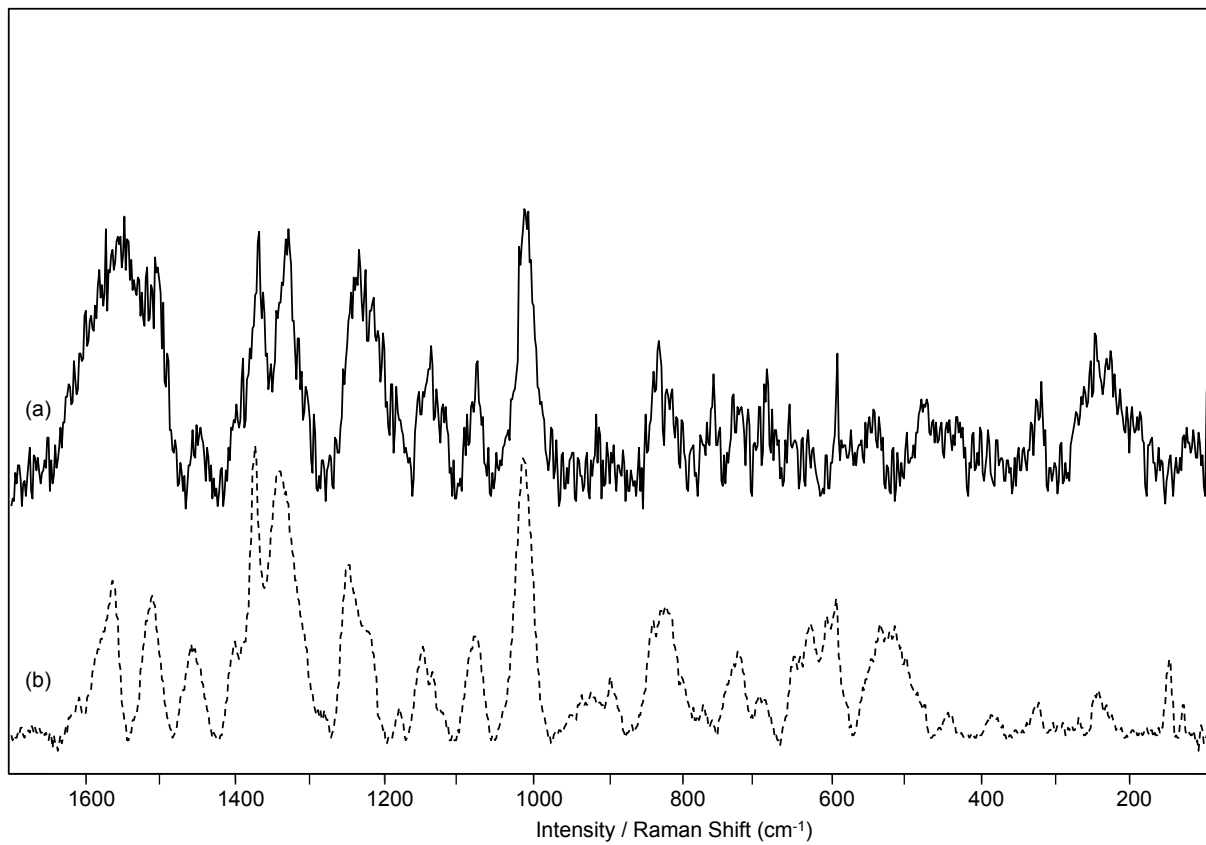


Figure 3

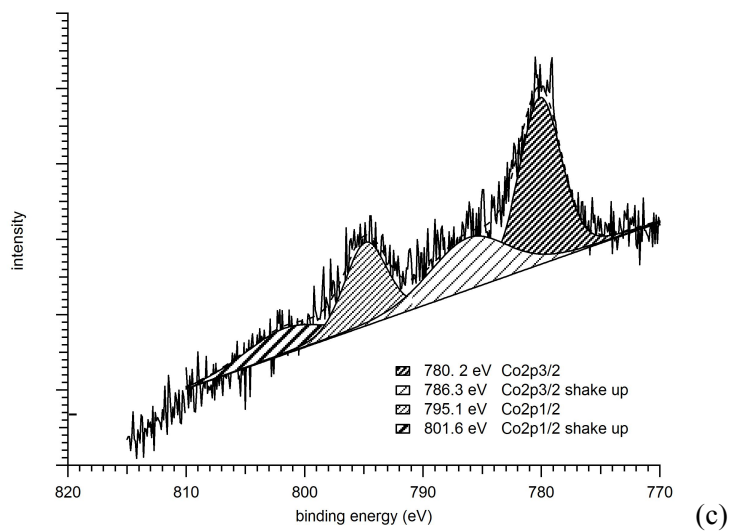
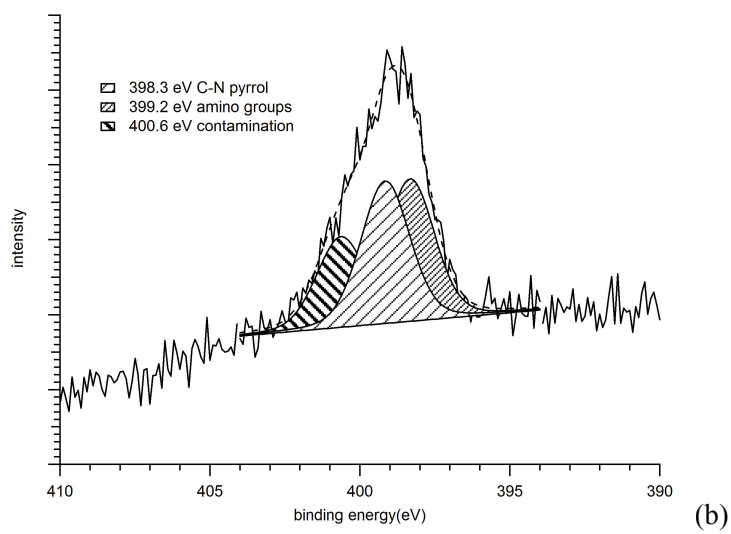
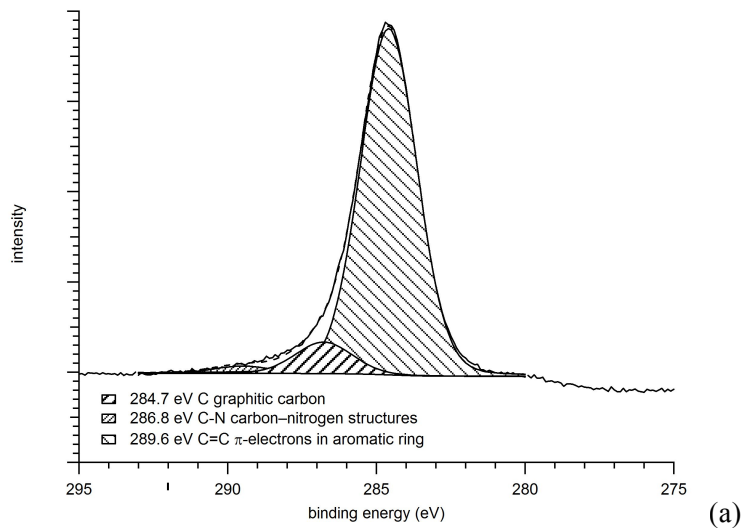


Figure 4

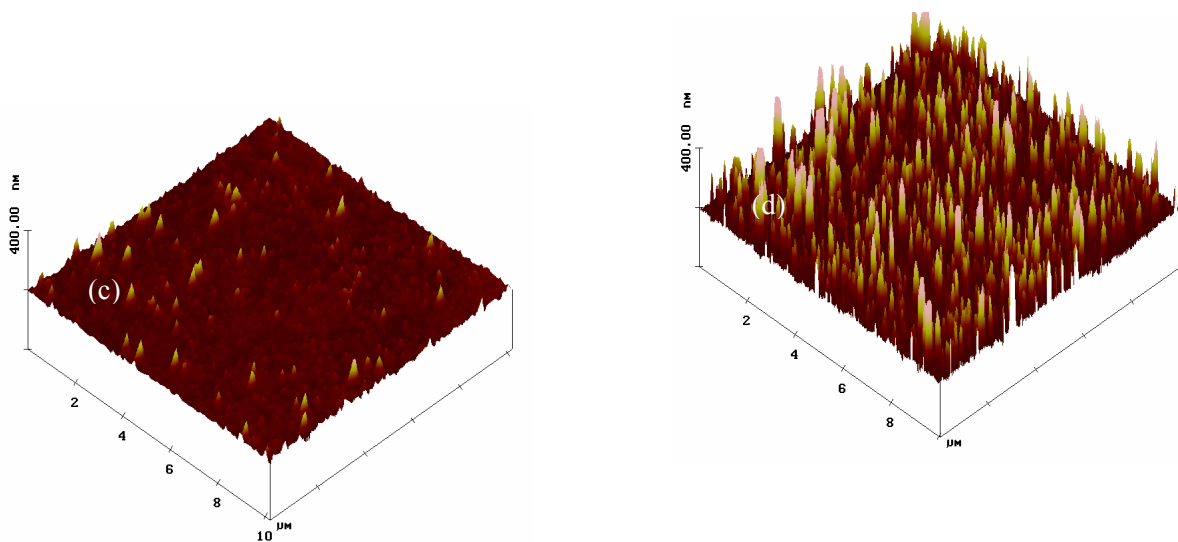
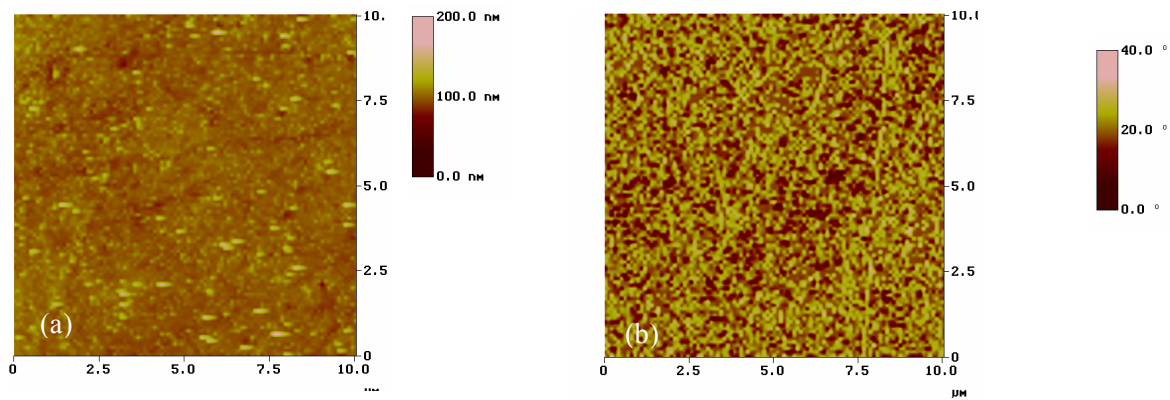


Figure 5

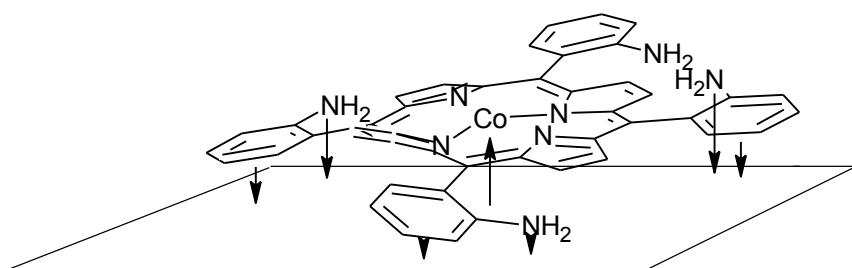


Figure 6

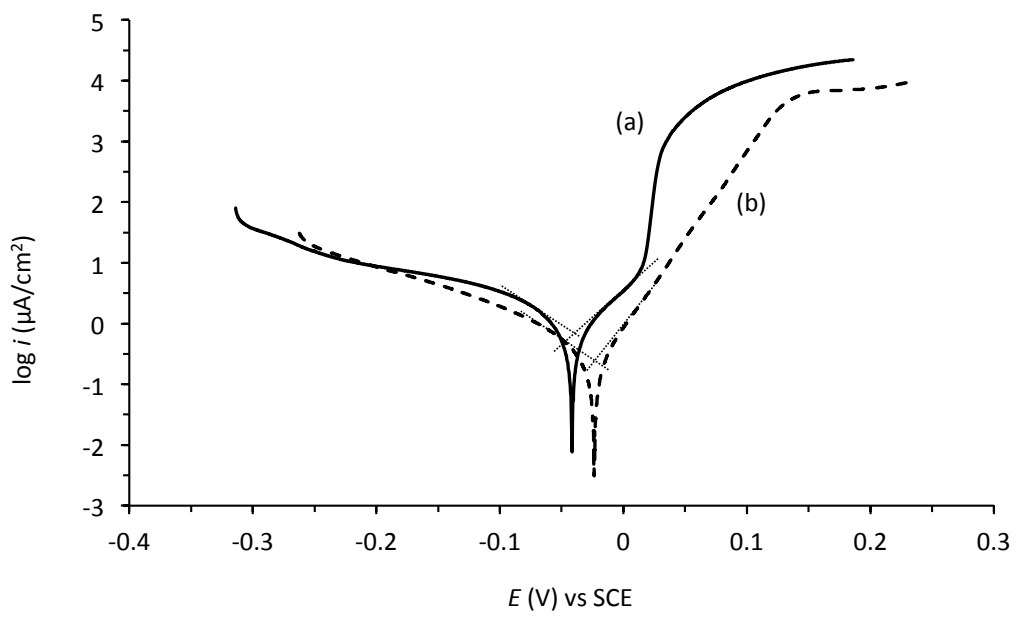


Figure 7

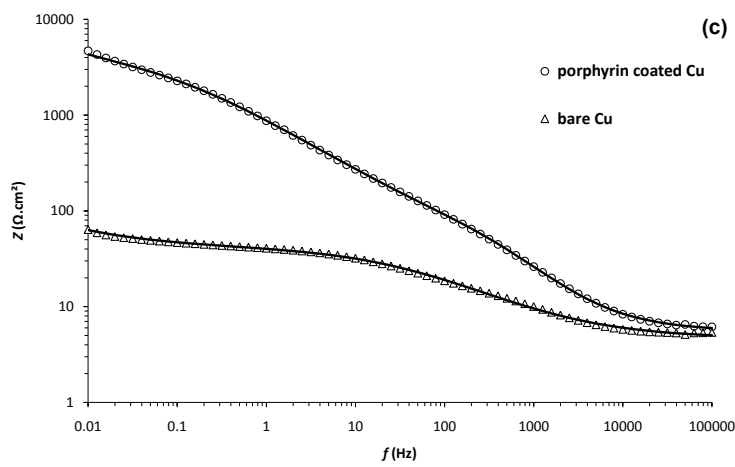
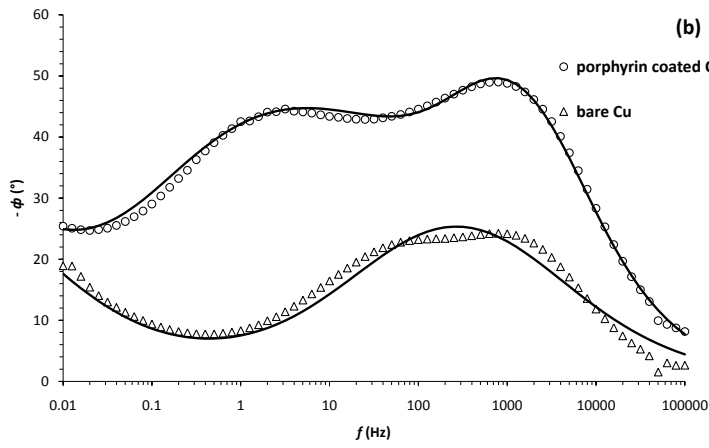
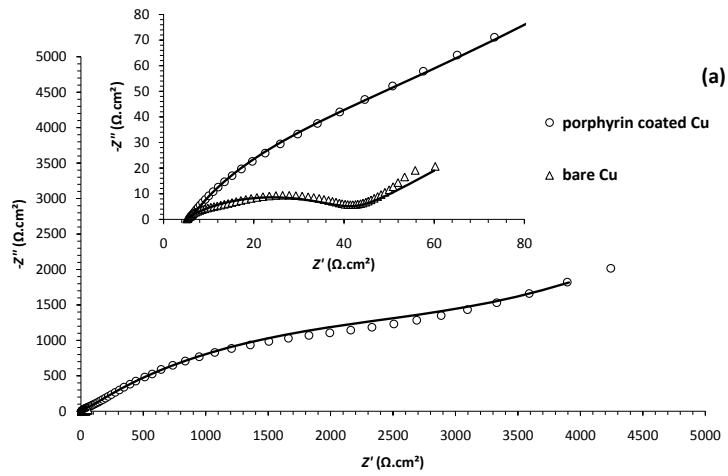


Figure 8

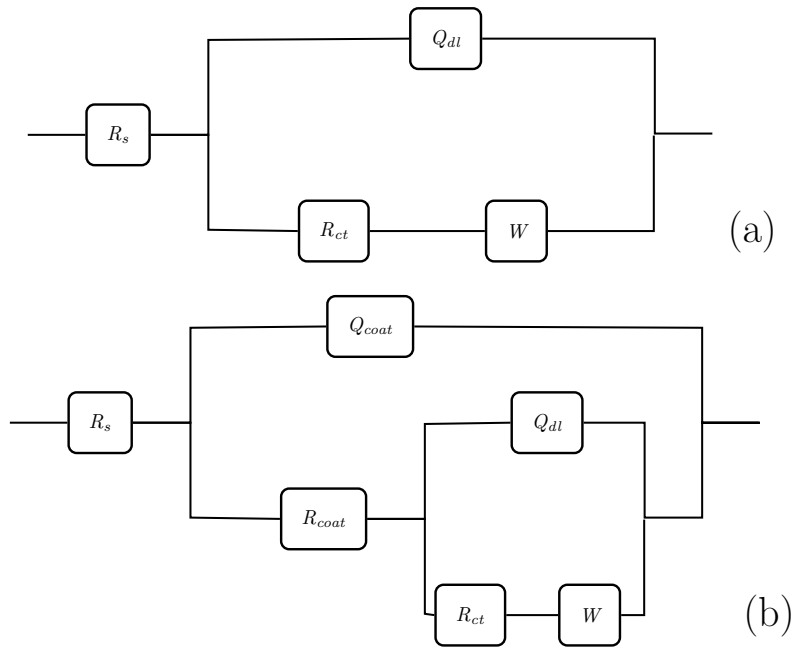


Figure 9